LETTER

Disentanglement of density and rotation dependences of the field penetration threshold on the J-TEXT tokamak

To cite this article: Zhuo Huang *et al* 2020 *Nucl. Fusion* **60** 064003

IOP Publishing | International Atomic Energy Agency Nuclear Fusion

Nucl. Fusion **60** (2020) 064003 (7pp) https://doi.org/10.1088/1741-4326/ab8859

Letter

Disentanglement of density and rotation dependences of the field penetration threshold on the J-TEXT tokamak

Zhuo Huang[1,2], Yunfeng Liang[1,2,3,b], Qiming Hu[4], Nengchao Wang[1,b], Da Li[1], Xiaoyi Zhang[1], Bo Rao[1], Zhipeng Chen[1], Song Zhou[1], Qi Zhang[1], Chengshuo Shen[1], Ying He[1], Yonghua Ding[1] and the J-TEXT team[a]

[1] International Joint Research Laboratory of Magnetic Confinement Fusion and Plasma Physics, State Key Laboratory of Advanced Electromagnetic Engineering and Technology, School of Electrical and Electronic Engineering, Huazhong University of Science and Technology, Wuhan 430074, China
[2] Forschungszentrum Jülich GmbH, Institut für Energie- und Klimaforschung—Plasmaphysik, Partner of the Trilateral Euregio Cluster (TEC), Jülich 52425, Germany
[3] Institute of Plasma Physics, Chinese Academy of Sciences, Hefei 230031, China
[4] Princeton Plasma Physics Laboratory, Princeton University, P.O. Box 451, NJ 08543, United States of America

E-mail: y.liang@fz-juelich.de and wangnc@hust.edu.cn

Received 17 January 2020, revised 7 April 2020
Accepted for publication 9 April 2020
Published 19 May 2020

Abstract

The field penetration threshold of magnetic perturbations has been observed to vary non-monotonically with an increase of density in ohmic plasmas on the J-TEXT tokamak. This observation appears contradicting the previous empirical density scaling law. Disentanglement of plasma density and rotation dependences of the field penetration threshold has been carried out. It shows that the field penetration threshold depends only weakly on the density but linearly on the plasma rotation. This result is not only important for the prediction of error field tolerance in fusion devices, but also opens a question on the role of density in the forced magnetic reconnection process in magnetized plasmas.

Keywords magnetohydrodynamics, magnetic reconnection, tearing instability, tokamaks

(Some figures may appear in colour only in the online journal)

Forced magnetic reconnection [1] in the presence of resonant magnetic perturbation (RMP), so called field penetration, is a fundamental issue in magnetically confined fusion plasmas. RMP is known for the profound effects on the plasma transport [2, 3] and magnetohydrodynamic (MHD) instabilities, i.e. locked mode and edge-localized-mode (ELM) suppression [4–7]. Field penetration in the plasma core triggers large magnetic islands which can cause degradation of plasma confinement and even a major disruption [8]. On the other hand, experimental evidences show that the transition from ELM mitigation to ELM suppression is due to the field penetration of RMP occurred at the plasma edge [9–11]. In addition, an upper limit of the operating window of RMP ELM suppression in tokamaks is determined by the disruptive field penetration threshold in the plasma core [12]. Understanding of the field penetration process, especially the parametric dependence of the field penetration threshold, is the basis of the RMP physics and application of RMP for the plasma control.

The parametric dependence of the field penetration threshold, especially on the plasma density, has been broadly

[a] See Liang *et al* 2019 (https://iopscience.iop.org/article/10.1088/1741-4326/ab1a72) for the J-TEXT team.
[b] Author to whom any correspondence should be addressed.

concerned and investigated for a long time due to its close connection with the start-up and early heating phase (L-mode, low density) in ITER [13]. An empirical scaling of the field penetration threshold is figured out by results in tokamaks in the form of $(b_r/B_T)_{crit} \propto n_e^{\alpha_n}$, where b_r is the field penetration threshold, B_T is the toroidal field, and n_e is the plasma density. However, the scaling coefficient α_n varies between different devices. The coefficient α_n is around 1 (linear) in JET [14], DIII-D [15], COMPASS-D [13], Alcator C-Mod [16], TEXTOR [17], and MAST [18], while being around 0.5 in COMPASS-C [19], J-TEXT [20], NSTX [21], and EAST [22]. One of the main obstacles in understanding the role of density is that some other parameters, which influence the field penetration threshold, vary with the variation of density. Plasma rotation is proven to play a critical role in the field penetration process due to the skin effect and the MHD stabilization effect [17, 23]. Researches in TEXTOR and LHD exhibited that the field penetration threshold was strongly related to the slip frequency (frequency difference of perturbed field and MHD mode) [24–26]. Results in JET took the plasma rotation (ω_0) into account in the empirical scaling as $(b_r/B_T)_{crit} \propto n_e^{\alpha_n}\omega_0^{\alpha_\omega}$ to clarify the α_n divergence and rotation dependence [27]. The α_n was modified to around 0.5 and no certain rotation dependence was concluded.

Predictions and optimizations for the error field tolerance in ITER have been performed based on empirical scalings [13, 28]. However, there are three cases which cannot be directly described by the empirical scaling. In NSTX, the field penetration threshold decreased when the density increased further in high-beta plasma. It was interpreted to be caused by the resonant field amplification (RFA) effects [21]. In TEXTOR, a sudden drop of the field penetration threshold was observed when the density kept increasing, and the density where this drop appeared moved with different fractions of momentum injections with and against the plasma current [29]. Previous researches on J-TEXT demonstrated that the field penetration threshold increases with the increase of density and scales proportionally to $n_e^{0.5}$ in the range of (0.7–2.7) $\times$ 10^{19} m^{-3} [20]. However, an unexpected lower field penetration threshold was recently observed in higher density plasma in a series of discharges [30]. Facts above show that the field penetration threshold can even decrease with an increase of the density in some cases, accentuating the question how the field penetration threshold depends on the density. This letter focuses on this problem based on a distinct result of field penetration experiments in J-TEXT, separates the plasma rotation from the density, and demonstrates a weak density dependence and a strong rotation dependence of the field penetration threshold.

J-TEXT is a circular, medium-sized, limiter tokamak with a major radius $R_0 = 105$ cm and a minor radius $a = 25$–29 cm [31]. 4 groups of coils are installed in the vacuum vessel to produce the resonant magnetic perturbations [32]. The dominant resonant component of the perturbed field is set as $m/n = 2/1$ (m and n are poloidal mode number and toroidal mode number, respectively) by adjusting the orientation of coil currents. The amplitude of the 2/1 component is calculated in vacuum at the last closed surface and has ratio of 0.25 mT kA^{-1} with the coil current. The experiment described in this letter is performed by applying the static 2/1 RMP onto an ohmically heated, L-mode plasma. No external momentum injection is applied in targeted plasmas. The plasma parameters are set to have a minor radius of 25.5 cm, a toroidal field of 1.7 T, a plasma current of 150 kA and an edge safety factor of 3.5. Figure 1(*a*) shows the field penetration thresholds for core line-averaged plasma densities $<n_e>$ in the range of (1–4.7) $\times$ 10^{19} m^{-3}. Interestingly there is an obvious non-monotonic dependence of the field penetration threshold on the density, violating the empirical density scaling. The density at the safety factor $q = 2$ resonant surface ($r/a = 0.8$) is shown in figure 1(*b*). It increases with the increase of core density as $n_e^{0.68}$. The non-monotonic dependence of the field penetration threshold can be also observed employing the density at the $q = 2$ resonant surface. Moreover, the ascending branch and the descending branch of the dependence curve are linked smoothly. It is different from the results in NSTX and TEXTOR [21, 29]. The sudden changes of the monotonicity of the density dependence in NSTX and TEXTOR could indicate a transition of mechanism.

Figure 2 shows the time evolution of two field penetration discharges with different densities but identical field penetration thresholds. Here the density is measured by the polarimeter-interferometer [33], the electron temperature (T_e) is measured by the electron cyclotron emission (ECE) radiometer [34], and the toroidal velocity of plasma rotation ($V_\emptyset$) is measured by the spectrometer filtered for Carbon V in the toroidal direction [35]. The occurrence time of the field penetration is set to 0 s, indicated by the vertical dashed line. Increases of the radial magnetic perturbation of $n = 1, 3, 5\ldots$ (mainly $n = 1$) components at 0 s indicate the excitation of the $n = 1$ locked mode (figure 2(*b*)). A reduction in density is observed at the time of the field penetration due to the confinement degradation effects of the locked mode (figure 2(*c*)). The temperature shows a sawtooth oscillation which disappears after the field penetration (figure 2(*e*)). The toroidal rotation decreases strongly in the direction of the ion diamagnetic drift after the field penetration (figure 2(*f*)). These common transitions in both discharges suggest the bifurcation of the plasma response to RMP from shielding to amplification. Interestingly, some differences between those two discharges can be also observed on the width of the induced locked modes and impacts on the plasma disruption.

Further information can be gleaned from comparison of parameters at the time of 0 s. The density in #1047742 is 1.43 $\times$ 10^{19} m^{-3} at the plasma core and 0.93 $\times$ 10^{19} m^{-3} at the $q = 2$ resonant surface, and it is 3.77 $\times$ 10^{19} m^{-3} at the plasma core and 1.83 $\times$ 10^{19} m^{-3} at the $q = 2$ resonant surface in #1047749. While the field penetration thresholds of both discharges are 4.4 kA (1.10 mT), even if their central line densities have ratio of 2.6. It is also observed that the plasma rotations at the $q = 2$ resonant surface measured before the field penetration from both low- and high-density discharges are fairly similar. This observation gives a hint that the plasma rotation may play a more significant role on the field penetration threshold rather than that of the plasma density.

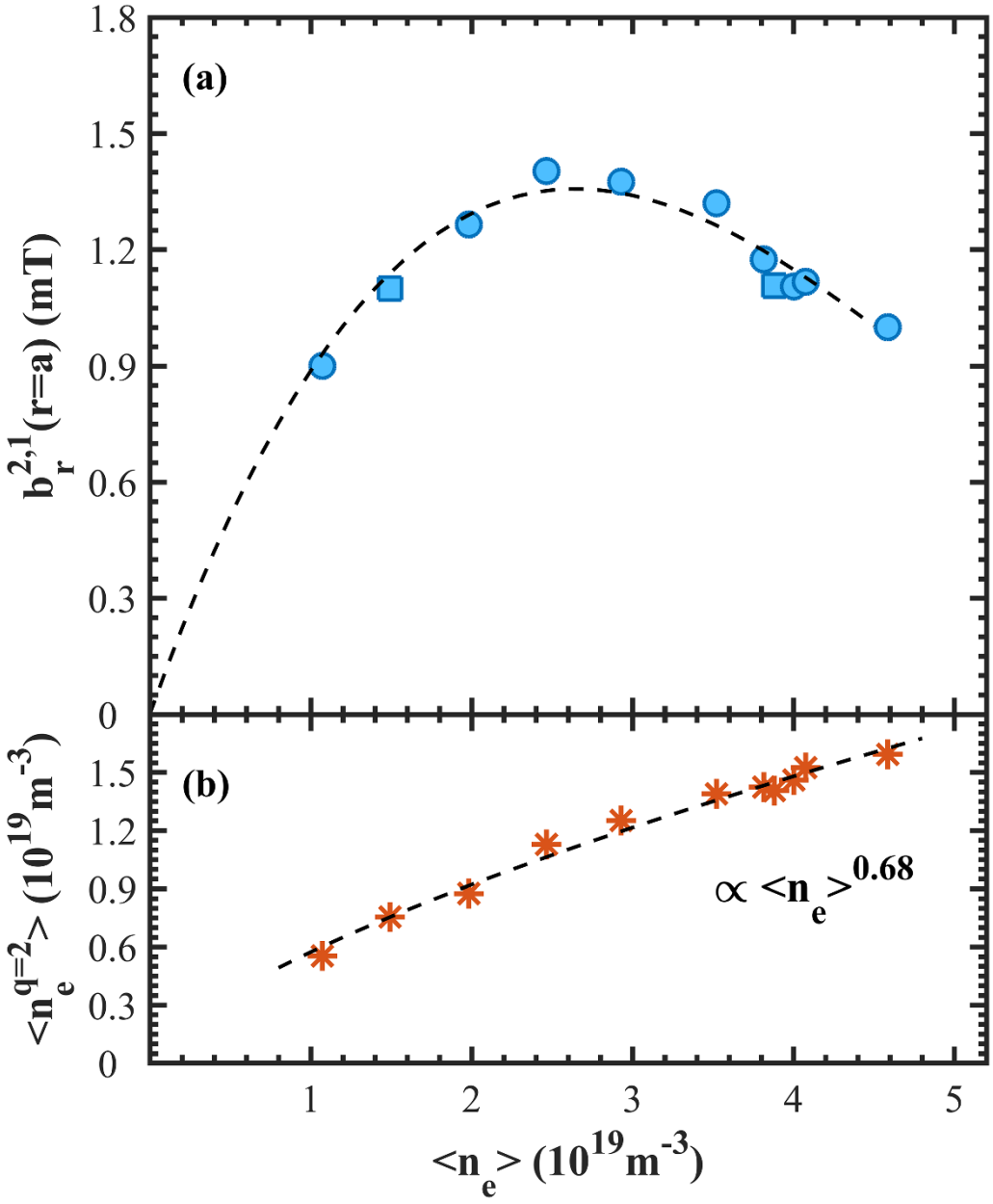

Figure 1. (*a*) Dependence of the field penetration threshold on the core line-averaged plasma density, fitted by a cubic polynomial as the dashed line. Two square symbols locate those discharges shown in figure 2. (*b*) line-averaged density at the $q = 2$ resonant surface.

The impact of the density on the plasma rotation has been investigated to clarify the role that the plasma rotation plays in the field penetration process. Figure 3 shows the toroidal rotation of plasma at the $q = 2$ resonant surface against the core density, as well as its comparison with the field penetration threshold. In this experiment with the static RMP applied, the slip frequency is determined by the MHD frequency. The MHD frequency is assumed to be the same as the frequency of the electron fluid [36]. It consists of the plasma rotation and the electron diamagnetic drift, expressed as

$$f_0 = \frac{nV_\emptyset}{2\pi R_0} + f_e^*, \tag{1}$$

where f_0 is the initial frequency of MHD and f_e^* is the electron diamagnetic frequency. The poloidal plasma rotation is neglected here [37]. The estimated f_e^* at the $q = 2$ resonant surface is 1 kHz, much smaller than the general MHD frequency (7–10 kHz) in J-TEXT [20]. Therefore, its contribution can be neglected and the slip frequency is mainly determined by the plasma rotation $V_\emptyset$. It can be observed in figure 3 that the plasma rotation is also non-monotonic with the increase of the density, showing a similar trend as the density dependence of field penetration threshold. This indicates that the non-monotonic density dependence of the field penetration is probably a consequence of the non- monotonic density dependence of the plasma rotation. Notice that the roll-over density of the plasma rotation is 3.06×10^{19} m^{-3}, and the roll-over density of the field penetration threshold is 2.47×10^{19} m^{-3}.

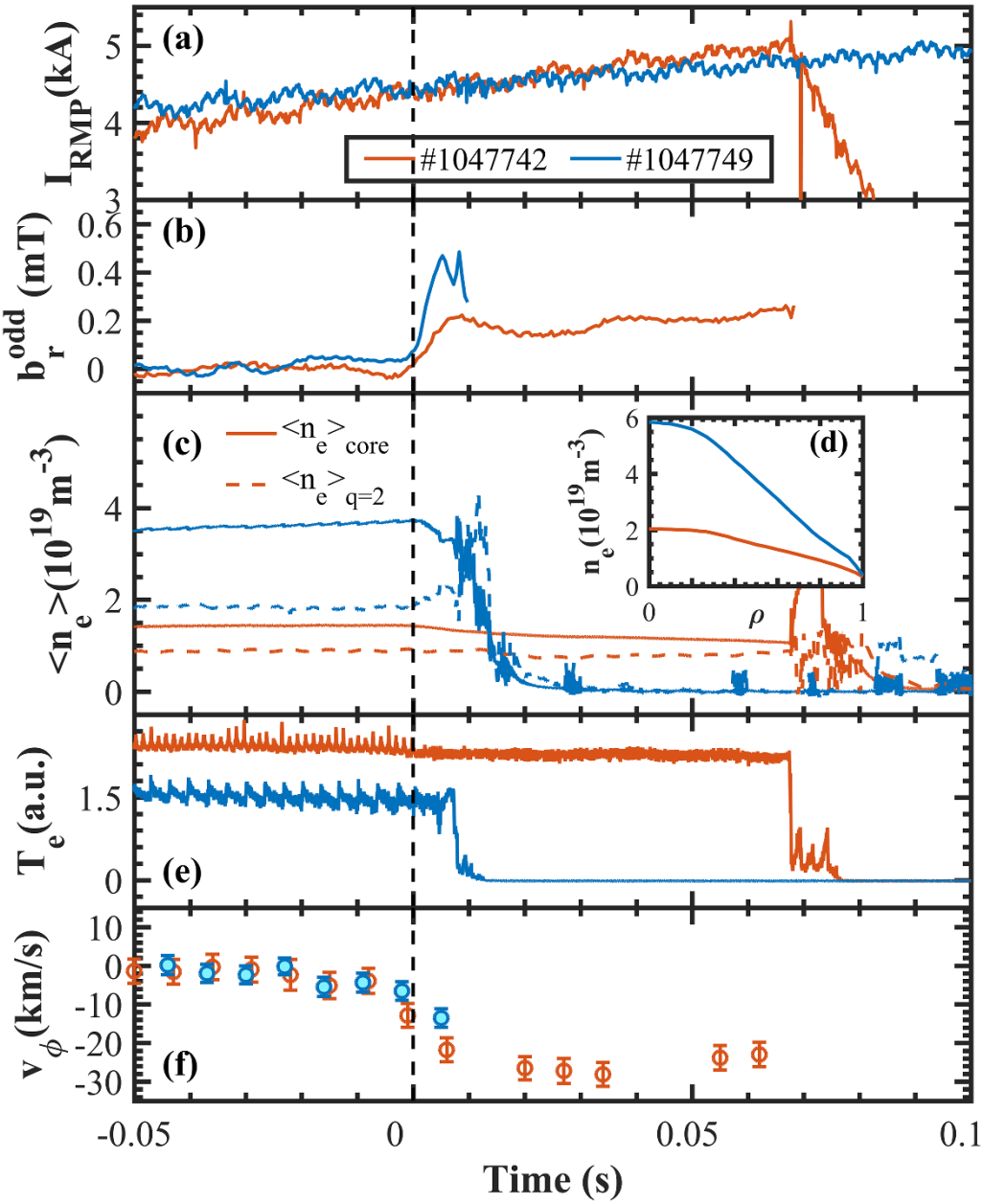

Figure 2. Time evolution of (*a*) plasma current, (*b*) radial perturbed field, (*c*) line-averaged density at the plasma core and $q = 2$ surface, (*e*) relative temperature at the plasma core, (*f*) toroidal rotation (direction of the electron diamagnetic drift is the positive direction). The occurrence time of the field penetration is set to 0 s. (*d*) Profiles of density at the time of 0 s inversed from the line-averaged density.

To investigate the effects of the plasma rotation on the field penetration threshold in different plasma conditions, two more series of field penetration discharges were performed with the controlled variable, plasma current, as 130 kA and 117 kA, corresponding to the edge safety factor (q_a) of 4.0 and 4.5, respectively. The non-monotonic density dependence of the field penetration threshold is observed in both conditions, so is the non-monotonic density dependence of the plasma rotation. Although the dependence curve of the field penetration threshold varies, it shows a similar shape as the dependence curve of the plasma rotation in corresponding condition. Here the roll-over density is employed to characterize these two dependence curve in different conditions as shown in figure 4. Roll-over densities of the plasma rotation in q_a of 4.0 and 4.5 conditions are 2.22×10^{19} m^{-3} and 1.91×10^{19} m^{-3}, decreasing with the increasing q_a. Similarly, roll-over densities of the field penetration threshold in q_a of 4.0 and 4.5 conditions are 1.88×10^{19} m^{-3} and 1.7×10^{19} m^{-3}, decreasing with the increasing q_a as well. This synergetic shift of roll-over densities in different conditions further demonstrates the close relationship between the plasma rotation and the field penetration threshold. Besides, the difference of the roll-over density is thought to come from other density-related effects which will be discussed later. The closer roll-over densities in higher q_a indicate that these density-related effects become weaker with the increase of q_a. It should be noted that the plasma rotation

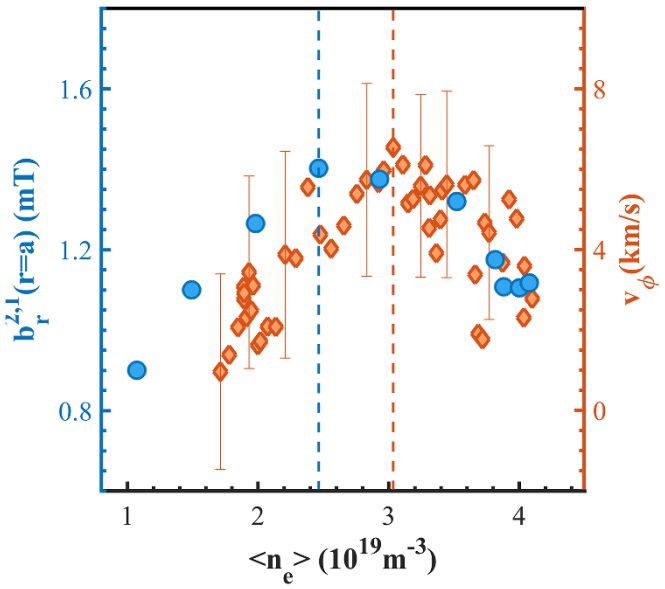

Figure 3. Comparison of the field penetration threshold and the plasma rotation. Roll-over densities are obtained where maximums of the plasma rotation and the field penetration threshold are located, indicated by vertical dashed lines.

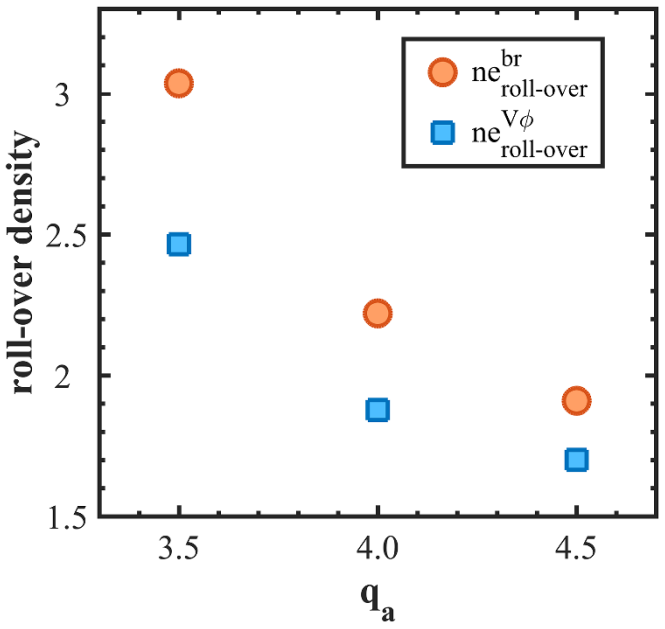

Figure 4. Comparison of the roll-over density between the field penetration threshold and the plasma rotation. It should be noted that the data points at the $q_a = 3.5$ are corresponding to the cases shown in figures 1–3.

in these experiments is sensitive to the plasma density due to the effect of ion-orbit loss [38]. In conclusion, facts above point to the density affecting the field penetration indirectly via its effects on the plasma rotation. This raises the question how important the density itself is for the field penetration threshold.

To separate the impact of the plasma rotation and the density on the field penetration threshold quantitatively, scaling is performed in terms of the plasma rotation and the density based on the data in figure 3. The observed field penetration threshold is fitted by the cubic polynomial shown in figure 1(*a*) and then scattered to the same sample as the plasma rotation. The MHD frequency is estimated from the measured plasma rotation by the experimental relationship as $f_0 = 0.3V_\emptyset + 8.5$(kHz, km s^{-1}) [39]. By logarithmic linearization of the scaling form $(b_r/B_T)_{crit} = Kn_e^{\alpha_n} f_0^{\alpha_f}$ (K is proportional coefficient and α_f is the coefficient of plasma rotation), one can obtain

$$\ln(b_r/B_T)_{crit} = \ln\mathrm{K} + \alpha_n \ln n_e + \alpha_f ln f_0. \tag{2}$$

The coefficient K, α_n, α_f can be figured out via the multiple linear regression by the data set of b_r, n_e, f_0. The non-monotonically varied plasma rotation holds strong nonlinearity with respect to the density. This guarantees the uniqueness and robustness of the fitting result. The resulting scaling is obtained as

$$(b_r/B_T)_{crit} \propto n_e^{-0.18\pm0.04} f_0^{1.04\pm0.25}. \tag{3}$$

Errors are the 95% confidence boundary. In the cases of $q_a = 4.0$ and $q_a = 4.5$, the obtained coefficient of plasma rotation α_f and plasma density α_n satisfy equation (3) within the error. The proportional coefficients K of $q_a = 3.5$, 4.0, and 4.5 cases are 0.85, 0.88, and 0.99, respectively. Equation (3) shows an almost linear dependence of the field penetration threshold on the plasma rotation. Single fluid MHD theory [40] exhibits regimes with the same linear dependence. It is also demonstrated by the numerical study [41] and the experimental observation [24]. Besides, equation (3) shows a negative and weak density dependence $n_e^{-0.18}$ of the field penetration threshold. It should be noted that, in these plasmas, the variation of the electron diamagnetic frequency at the $q = 2$ surface is estimated to be within 1.5 kHz. When taking into account the dependence of the diamagnetic frequency on the density, the weak density dependence and linear rotation dependence of the field penetration threshold can be still observed from the scaling analysis. A comparison of the field penetration threshold between the experimental observation and the prediction based on the scaling equation (3) in the case of $q_a = 3.5$ with the measured plasma rotation and density is shown in figure 5. The dotted line in figure 5 shows the density trace. The field penetration threshold increases from 1.1 mT to 1.4 mT and then decreases from 1.4 mT to around 1.2 mT along the dotted line with the increase of density. Here, the experimental data used in figure 5 is corresponding to that plotted in figure 3. Similar to the principle of the Lissajous curve [42], the close trajectories of the ascending branch and descending branch shown in figure 5 indicate that there is no phase difference (roll-over density difference) between the predicted threshold and the experimental threshold. It indicates that the slight difference of roll-over densities between the plasma rotation and the field penetration threshold (figure 3) is caused by the weak negative density dependence.

This density dependence $n_e^{-0.18}$ is completely different from the previous positive and strong dependence ($n_e^{0.5}$ and n_e^1) in the empirical scaling. J-TEXT exhibits the $n_e^{0.5}$ scaling

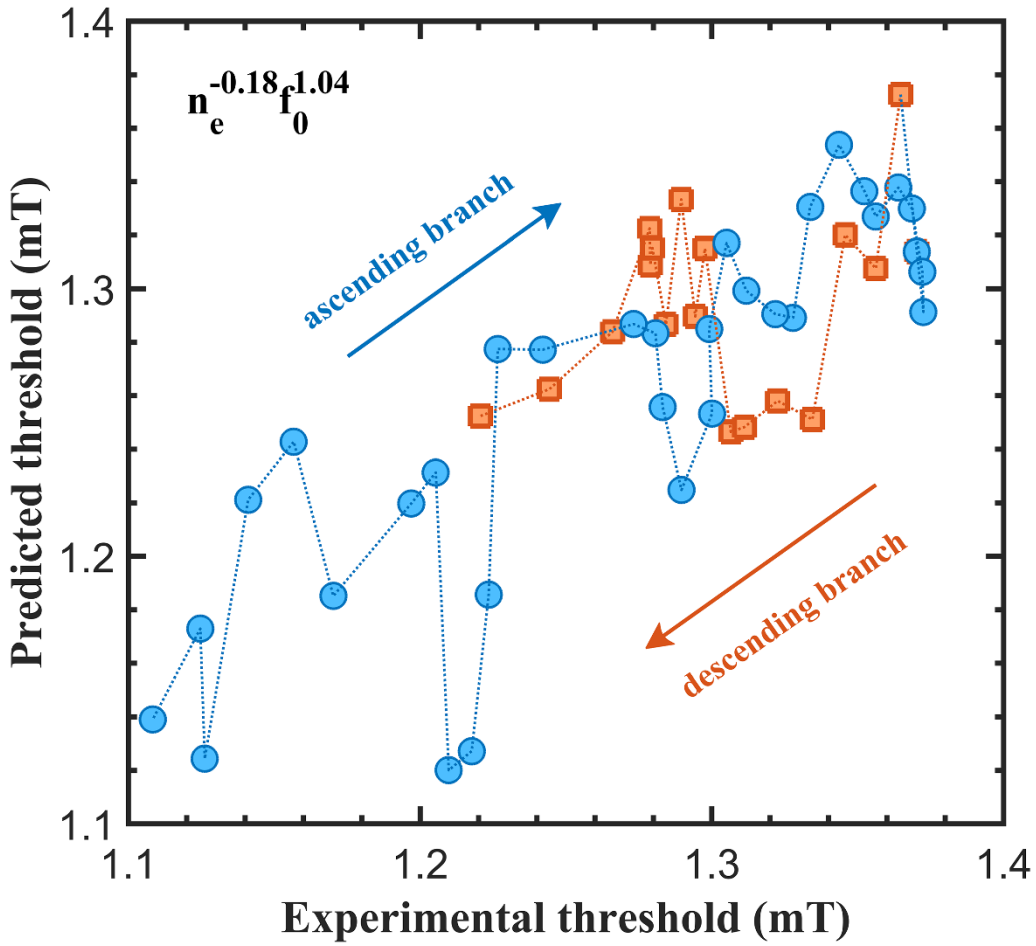

Figure 5. Comparison of the field penetration threshold between the experimental observation and prediction in the condition of $q_a = 3.5$. The corresponding density of each point increases along the dotted line. Trajectories are classified by the increasing threshold from 1.1 mT to 1.4 mT (ascending bracnch) and decreasing threshold from 1.4 mT to around 1.2 mT (descending branch).

before entering a high density region ((2.7–4.3) $\times$ 10^{19} m^{-3}) where the non-monotonicity appears in the density dependence of the plasma rotation. The empirical scaling for other machines might be similarly affected and a non-monotonic density dependence of the field penetration might appear as well in an expanded density range. The observed non-monotonic field penetration threshold here is beneficial for the clarification of the impacts of the density from other factors. Moreover, it is hard to say that the weak density dependence $n_e^{-0.18}$ is a direct physical effect of density. Theory indicates that there are different regimes of the field penetration related to plasma parameters [40]. Work in [22] derived a general form of the field penetration threshold in different regimes as $(b_r/B_T)_{crit} \propto n_e^{\alpha_n} \tau_V^{-\alpha_n} T_e^{\alpha_T} f_0^{\alpha_f}$. Here τ_V is the viscosity diffusion time. A possible explanation of the experimental density dependence is the following: The dependence $\tau_v \propto n_e$ is derived employing the Neo-Alcator scaling [40, 43], so no density dependence of the field penetration threshold should be observed in principle. The $n_e^{-0.18}$ density dependence might be due to an effect of the plasma temperature. It is observed in the experiment that the temperature decreases with the increase of the density according to the relationship $T_e \propto n_e^{-0.63\pm0.24}$ as shown in figure 6. Combining with equation (3) and the relationship of density at the $q = 2$ surface (figure 1(*b*)), one can obtain the scaling as $(b_r/B_T)_{crit} \propto T_e^{0.39} f_0^{1.04}$, approximately consistent with the Rutherford regime and Transition regime [22, 40].

In these experiments, the low-density region ($n_e < 1.0 \times 10^{19}$ m^{-3}) was not investigated due to the operational limits of J-TEXT. It does not rule out that the previous empirical density scaling of the field penetration threshold may be still availed at the low density as a problematic regime in driving the locked mode. Besides, due to lack of external momentum injection methods on J-TEXT, the field penetration threshold was not possible investigated in a large range of plasma rotation and with different rotation generation mechanisms. Future work to clarify the role of the plasma density and rotation in the field penetration threshold in a larger operational domain is needed.

In summary, experiments of the m/n = 2/1 field penetration were performed in ohmic plasmas on the J-TEXT tokamak. The field penetration threshold was observed to vary non-monotonically with the increase of density. This is different from most of the previous results and can not be accommodated into the empirical density scaling. With the disentanglement of density and rotation dependences carried out, it

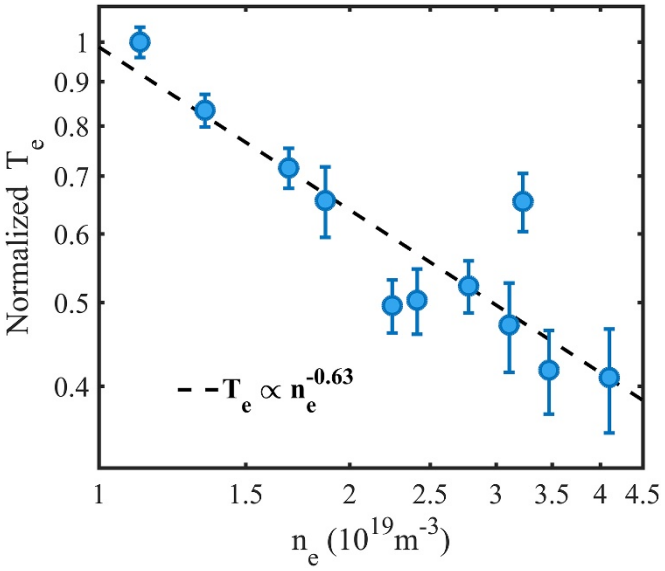

Figure 6. Dependence of the relative electron temperature on the plasma density in the case of the $q_a = 3.5$.

is revealed that there is only a weak or even no dependence of the field penetration threshold on the density and a linear dependence on the plasma rotation. This result is not only fundamentally important for the prediction of error field tolerance in magnetically confined fusion devices, but also opens a question on the role of density in the forced magnetic reconnection process in magnetized plasmas.

Acknowledgment

This work is supported by the National MCF Energy R&D Program of China (No. 2018YFE0309100), the National Key R&D Program of China (No. 2017YFE0301100), and the National Natural Science Foundation of China (Nos. 51821005 and 11905078).

ORCID iDs

Zhuo Huang https://orcid.org/0000-0001-7527-6464
Qiming Hu https://orcid.org/0000-0002-8877-4988
Nengchao Wang https://orcid.org/0000-0001-6797-2398
Zhipeng Chen https://orcid.org/0000-0002-8330-0070

References

[1] Sato T. and Hayashi T. 1979 *Phys. Fluids* **22** 1189
[2] Liang Y. *et al* 2005 *Phys. Rev. Lett.* **94** 105003
[3] Hu Q. *et al* 2014 *Nucl. Fusion* **54** 064013
[4] Evans T. *et al* 2004 *Phys. Rev. Lett.* **92** 235003
[5] Evans T.E. *et al* 2006 *Nat. Phys.* **2** 419
[6] Liang Y. *et al* 2007 *Phys. Rev. Lett.* **98** 265004
[7] Liang Y., Gimblett C., Browning P., Devoy P., Koslowski H., Jachmich S., Sun Y. and Wiegmann C. 2010 *Phys. Rev. Lett.* **105** 065001
[8] Hender T., Wesley J. and Bialek J. 2007 Progress in the ITER Physics Basis Chapter 3: MHD stability, operational limits and disruptions *Nucl. Fusion* **47** S128
[9] Kirk A., Harrison J., Liu Y., Nardon E., Chapman I. and Denner P. 2012 *Phys. Rev. Lett.* **108** 255003
[10] Nazikian R. *et al* 2015 *Phys. Rev. Lett.* **114** 105002
[11] Sun Y. *et al* 2016 *Phys. Rev. Lett.* **117** 115001
[12] Park J.-K. *et al* 2018 *Nat. Phys.* **14** 1223
[13] Buttery R. *et al* 1999 *Nucl. Fusion* **39** 1827
[14] Buttery R., De'Benedetti M., Hender T. and Tubbing B. 2000 *Nucl. Fusion* **40** 807
[15] Scoville J.T., La Haye R.J., Kellman A.G., Osborne T.H., Stambaugh R.D., Strait E.J. and Taylor T.S. 1991 *Nucl. Fusion* **31** 875
[16] Wolfe S.M. *et al* 2005 *Phys. Plasmas* **12** 056110
[17] Wolf R.C. *et al* 2005 *Nucl. Fusion* **45** 1700
[18] Howell D.F., Hender T.C. and Cunningham G. 2007 *Nucl. Fusion* **47** 1336
[19] Hender T. *et al* 1992 *Nucl. Fusion* **32** 2091
[20] Wang N. *et al* 2014 *Nucl. Fusion* **54** 064014
[21] Park J.-K., Menard J.E., Gerhardt S.P., Buttery R.J., Sabbagh S.A., Bell R.E. and LeBlanc B.P. 2012 *Nucl. Fusion* **52** 023004
[22] Wang -H.-H. *et al* 2018 *Nucl. Fusion* **58** 056024
[23] Kikuchi Y. *et al* 2006 *Phys. Rev. Lett.* **97** 085003
[24] Koslowski H.R., Liang Y., Krämer-Flecken A., Löwenbrück K., Hellermann M.V., Westerhof E., Wolf R.C., Zimmermann O. and the TEXTOR team 2006 *Nucl. Fusion* **46** L1
[25] De Bock M., Classen I., Busch C., Jaspers R., Koslowski H., Unterberg B. and the TEXTOR Team 2008 *Nucl. Fusion* **48** 015007
[26] Watanabe K., Sakakibara S., Narushima Y., Ohdachi S., Suzuki Y., Takemura Y., Ida K., Yoshinuma M. and Yamada I. 2019 *Nucl. Fusion* **59** 086049
[27] Lazzaro E. *et al* 2002 *Phys. Plasmas* **9** 3906
[28] Park J.-K., Boozer A.H., Menard J.E. and Schaffer M.J. 2008 *Nucl. Fusion* **48** 045006
[29] Loewenbrueck K. *et al* 2007 Density dependence of the tearing mode threshold *Proc. 34th EPS Conf. on Plasma Physics (Warsaw, Poland, 2–6 July 2007)* vol 31F (ECA) P1.136 (http://epsppd.epfl.ch/Warsaw/pdf/P1_136.pdf)
[30] Hu Q., Wang N., Yu Q., Ding Y., Rao B., Chen Z. and Jin H. 2015 *Plasma Phys. Control. Fusion* **58** 025001
[31] Liang Y. *et al* 2019 *Nucl. Fusion* **59** 112016
[32] Rao B. *et al* 2014 *Fusion Eng. Des.* **89** 378
[33] Chen J. *et al* 2014 *Rev. Sci. Instrum.* **85** 11D303
[34] Yang Z.J., Phillips P.E., Zhuang G., Xiao J.S., Huang H., Rowan W.L. and Wang Z.J. 2012 *Rev. Sci. Instrum.* **83** 10e313
[35] Cheng Z.F., Luo J., Wang Z.J., Zhang Z.P., Zhang X.L., Hou S.Y., Cheng C. and Zhuang G. 2013 *Rev. Sci. Instrum.* **84** 073508
[36] Klüber O., Zohm H., Bruhns H., Gernhardt J., Kallenbach A. and Zehrfeld H.P. 1991 *Nucl. Fusion* **31** 907
[37] Stix T.H. 1973 *Phys. Fluids* **16** 1260
[38] Zeng Z. *et al* 2018 *Nucl. Fusion* **58** 076001
[39] Yan W. *et al* 2018 *Plasma Phys. Control. Fusion* **60** 035007
[40] Fitzpatrick R. 2012 *Plasma Phys. Control. Fusion* **54** 094002
[41] Waelbroeck F. 2009 *Nucl. Fusion* **49** 104025
[42] Al-Khazali H.A. and Askari M.R. 2012 *IOSR J. Eng.* **2** 971
[43] Simmet E.E. and the ASDEX team 1996 *Plasma Phys. Control. Fusion* **38** 689